

SMALL- x BEHAVIOR OF THE SLOPE $d\ln F_2/d\ln(1/x)$ IN THE PERTURBATIVE QCD FRAMEWORK

A. V. Kotikov^{*}

*Bogoliubov Laboratory of Theoretical Physics
Joint Institute for Nuclear Research
141980, Dubna, Russia*

G. Parente^{**}

*Departamento de Física de Partículas
Universidade de Santiago de Compostela
15706, Santiago de Compostela, Spain*

Submitted 8 April 2003

In the leading twist approximation of the Wilson operator product expansion, we show that using an analytic parameterization for the behavior of the x slope of the structure function F_2 at small x in perturbative QCD and applying a flat initial condition in the DGLAP evolution equations leads to a very good agreement with the new precise deep inelastic scattering experimental data from HERA.

PACS: 13.60.Hb, 12.38.Bx

1. INTRODUCTION

Measurements of the deep inelastic scattering structure function F_2 [1–3], and of the derivatives $dF_2/d\ln(Q^2)$ [1, 2, 4] and $d\ln F_2/d\ln(1/x)$ [4, 5] in HERA have allowed accessing a very interesting kinematical range for testing theoretical ideas on the behavior of quarks and gluons [6] carrying a very low fraction of the proton momentum, the so-called small- x region. In this limit, one expects that nonperturbative effects can give essential contributions. However, a reasonable agreement between the HERA data and the next-to-leading approximation of perturbative QCD has been observed for $Q^2 \geq 2 \text{ GeV}^2$ (see review [7] and references therein), and therefore perturbative QCD can describe the evolution of F_2 and its derivatives down to very low Q^2 values, traditionally explained by soft processes. It is fundamentally important to find the kinematical region where the well-established perturbative QCD formalism can be safely applied at small x .

The standard program to study the x behavior of quarks and gluons is carried out by comparison of data with the numerical solution of the Dokshitzer–Gribov–Lipatov–Altarelli–Parisi (DGLAP)¹⁾ equations [8] by fitting the parameters of the x profile of partons at some initial Q_0^2 and the QCD energy scale Λ [10, 11]. But for analyzing the small- x region exclusively, there is the alternative of a simpler analysis using some of the existing analytic solutions of the DGLAP equations in the small- x limit [12–15]. This was done in Ref. [12], where it was pointed out that the HERA small- x data can be interpreted in terms of the so-called doubled asymptotic scaling phenomenon related to the asymptotic behavior of the DGLAP evolution discovered many years ago [16].

The study in Ref. [12] was extended in Ref. [13–15] to include the finite parts of anomalous dimensions of Wilson operators and Wilson coefficients²⁾. This has

^{*}E-mail: kotikov@thsun1.jinr.ru; present address: Institut für Theoretische Teilchenphysik, Universität Karlsruhe, D-76128, Karlsruhe, Germany.

^{**}E-mail: gonzalo@gaes.usc.es

¹⁾ At small x , there is a different approach based on the Balitsky–Fadin–Kuraev–Lipatov (BFKL) equation [9], whose application is out of the scope of this paper. However, we sometimes use the BFKL-based predictions below in discussions and for comparison with our results in the generalized doubled asymptotic scaling approximation.

²⁾ In the standard doubled asymptotic scaling approximation [16], only the singular parts of the anomalous dimensions are used.

led to the prediction [14, 15] of the small- x asymptotic form of parton distributions in the framework of the DGLAP equation starting at some Q_0^2 with the flat function

$$f_a(Q_0^2) = A_a, \quad (1)$$

where f_a are the parton distributions multiplied by x , A_a are unknown parameters to be determined from data, and $a = q, g$ hereafter.

We refer to the approach in Ref. [13–15] as the generalized doubled asymptotic scaling approximation. In the generalized doubled asymptotic scaling approximation, the flat initial conditions in Eq. (1) determine the basic role of the singular parts of anomalous dimensions, as in the standard case [12], while the contribution from finite parts of anomalous dimensions and from Wilson coefficients can be considered as corrections, which are however important for a better agreement with experimental data [14]. In the present paper, similarly to Refs. [12–15], we neglect the contribution from the nonsinglet quark component.

The use of the flat initial condition given in Eq. (1) is supported by the actual experimental situation: the low- Q^2 data [1, 4, 17, 18] are well described for $Q^2 \leq 0.4 \text{ GeV}^2$ by the Regge theory with the Pomeron intercept

$$\alpha_P(0) \equiv \lambda_P + 1 = 1.08,$$

close to the standard one ($\alpha_P(0) = 1$). The small rise observed in the HERA data [1, 2, 4, 18, 19] at low Q^2 can be naturally explained by including higher twist terms (see [15, 20]). Moreover, HERA data [1, 2, 18, 19] with $Q^2 > 1 \text{ GeV}^2$ are in good agreement with the predictions from the Gluck–Reya–Vogt (GRV) parton densities [11], which supports our aim to develop the analytic form for the parton densities at small x because at least conceptually, our method is very close to the GRV approach.

The purpose of this paper is to extend the study in Ref. [14] to compare the predictions from the generalized doubled asymptotic scaling approach with the new precise H1 data [5] for the F_2 slope. The paper is organized as follows. In Sec. 2, we address the present situation with experimental data for the slope $d \ln F_2 / d \ln(1/x)$ and briefly review some approaches to describe them. For completeness, Secs. 3 and 4 contain a compilation of the basic formulas in the generalized doubled asymptotic scaling approximation from Ref. [14] needed for the present study. In Sec. 5, we compare our predictions for the derivative $d \ln F_2 / d \ln(1/x)$ with the experimental data and discuss the obtained results.

2. THE SLOPE $d \ln F_2 / d \ln(1/x)$: EXPERIMENTAL DATA AND QCD PHENOMENOLOGY

Various groups have been able to fit the available data (mostly separating the low- and high- Q^2 regions) using a steep input at small x , $x^{-\lambda}$, $\lambda > 0$. This is clearly different from the flat input in the doubled asymptotic scaling approach of Refs. [12–15], also describing the experimental results reasonably well. In some sense, this is not very surprising because the modern HERA data (at large Q^2) cannot distinguish between the behavior from a steep input parton parameterization at quite large Q^2 and the steep form acquired after dynamical evolution from a flat initial condition at quite low values of Q^2 .

Moreover, for the Q^2 -evolution based on the full set of anomalous dimensions obtained at $x \rightarrow 0$ in Ref. [21] within the Balitsky–Fadin–Kuraev–Lipatov (BFKL) formalism [9], the results weakly depend on the form of the initial condition [22], preserving the steep ones and changing the flat ones. In working with anomalous dimensions at a fixed order in α_s , the initial conditions are important when the data are considered in a wide Q^2 range and it is necessary to adequately choose the form of the parton distribution asymptotic form at some Q_0^2 .

As discussed in the Introduction, the use of a flat initial condition leads to the (generalized) doubled asymptotic scaling approximation [13–15]. An alternative to this is the choice of a steep initial condition at some sufficiently large Q_c^2 ,

$$f_a(x, Q_c^2) \propto x^{-\lambda_c}$$

(the subscript c stands for constant), which leads to the Q^2 -dependence of $f_a(x, Q^2)$ [23–27] given by (for $x^{-\lambda_c} \gg \text{const}$)

$$\frac{f_a(x, Q^2)}{f_a(x, Q_c^2)} \sim \frac{M_a^+(1 + \lambda_c, Q^2)}{M_a^+(1 + \lambda_c, Q_c^2)}, \quad (2)$$

where $M_a^+(1 + \lambda_c, Q^2)$ is the analytic continuation (from integer n to real $1 + \lambda_c$) of the «+» component of the Mellin moment of $f_a(x, Q^2)$,

$$M_a(n, Q^2) = \int_0^1 dx x^{n-2} f_a(x, Q^2). \quad (3)$$

For $x^{-\lambda_c} \gg \text{const}$, the slope λ_c must be Q^2 -independent [24, 25] and the whole Q^2 -dependence of $f_a(x, Q^2)$ comes from the factor $M_a^+(1 + \lambda_c, Q^2)$ in front of $x^{-\lambda_c}$ in Eq. (2). Approximations similar to

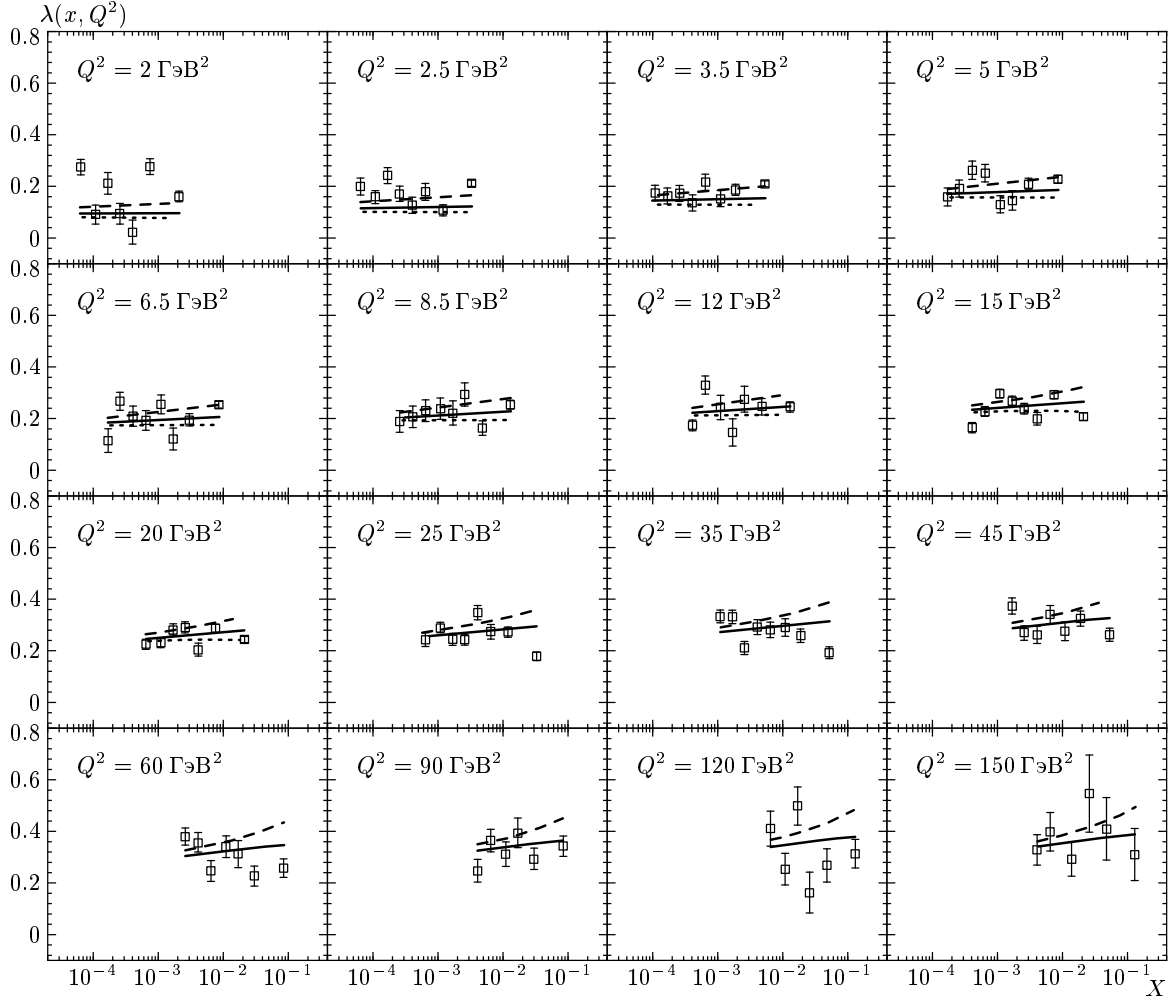


Fig. 1. The derivative $d \ln F_2 / d \ln(1/x)$ (the effective slope λ) as a function of x for different values of Q^2 . Data points are from H1 [5]. Only statistical uncertainties are shown. The solid line is the result of a fit using $\lambda_{F_2}^{eff}$ in Eq. (15) with fixed $Q_0^2 = 1 \text{ GeV}^2$ and $x_0 = 1$. The dotted line is the same but with the parameters from a fit to the F_2 data in Ref. [14]. The dashed line corresponds to the asymptotic expression $\lambda_{F_2}^{eff,as}$ in Eq. (16)

Eq. (2) have been successfully applied in studying the Q^2 -dependence of HERA data at large Q^2 (see Ref. [28] and references therein).

Considering the low- Q^2 region separately, it is also possible to have a good agreement between the F_2 data and its Regge-like behavior [4]. Indeed, at $Q^2 \rightarrow 0$, F_2 can be determined by the relation

$$F_2 = \frac{Q^2}{4\pi\alpha_{em}} \sigma_{tot}^{\gamma^*p}, \quad (4)$$

where α_{em} is the electromagnetic coupling constant and $\sigma_{tot}^{\gamma^*p}$ is the total (virtual) photoproduction cross section.

A large amount of experimental data on hadronic

cross sections for many different processes show a universal rise at large energies, which allows parameterizing all these cross sections as the sum of two different components

$$\sigma_{tot}^{\gamma^*p} = A_P s^{\alpha_P(0)-1} + A_R s^{\alpha_R(0)-1}, \quad (5)$$

where s is the center-of-mass energy squared. The constants A_P and A_R are process-dependent magnitudes and the intercepts $\alpha_P(0) \approx 1.08$ and $\alpha_R(0) \approx 0.5$ (see [29]) are universal process-independent constants. The first and second terms in Eq. (5) correspond to (soft) Pomeron and Reggeon exchange, respectively.

From Eqs. (4) and (5), we immediately obtain that as $Q^2 \rightarrow 0$,

$$F_2(x, Q^2) \propto x^{-\varepsilon},$$

and hence

$$f_a(x, Q^2) \propto x^{-\varepsilon}, \quad \varepsilon = \alpha_P(0) - 1 \approx 0.08$$

because $s = Q^2/x$ at small x .

There have been many attempts to study the entire Q^2 region in the Regge-asymptotic framework (see, e.g., the reviews in Ref. [7]). The reports in Ref. [7] contain a great number of models, but we restrict ourselves to only two of them.

In Ref. [30], the fit to F_2 experimental data was sought with

$$f_a(x, Q^2) \propto x^{-\lambda(Q^2)}, \quad (6)$$

and rapidly changing $\lambda(Q^2)$ was found in the transition range $Q^2 \sim 5\text{--}10 \text{ GeV}^2$. Unfortunately, it is rather difficult to reconcile the Regge-like behavior given by Eq. (6) with DGLAP evolution in the entire Q^2 range. Some progress along this line achieved in Ref. [27] is also based on the flat initial conditions given by Eq. (1). But the parton distribution structure in Ref. [27] is limited by the Regge-like form of Eq. (6), which allows reconciling it with DGLAP evolution only separately at low Q^2 , where $\lambda(Q^2)$ is close to 0 (or to ε), and at large Q^2 , where $\lambda(Q^2) \sim \lambda_c$. The structure function F_2 and parton distributions were obtained in Ref. [27] for the entire Q^2 range only as a combination of these two representations.

For other types of models (see [32, 33]), the phenomenological Q^2 -dependence of $\lambda(Q^2)$ is given by

$$\lambda(Q^2) = \varepsilon \left(1 + \frac{Q^2}{Q^2 + c} \right)$$

with a fitted constant c . This produces soft values of the slope $\lambda(Q^2)$ close to ε at low Q^2 and hard ones, $\lambda(Q^2) \sim \lambda_c \sim 0.2\text{--}0.3$, at $Q^2 \geq 20 \text{ GeV}^2$.

New precise experimental data on $\lambda(Q^2)$ have become available very recently [5]. The H1 data points are shown in Fig. 1, where one can observe that for a fixed Q^2 , λ is independent of x in the range $x < 0.01$ within the experimental uncertainties. Indeed, H1 data are well described by the power behavior [5]

$$F_2(x, Q^2) = Cx^{-\lambda(Q^2)}, \quad (7)$$

where

$$\lambda(Q^2) = \hat{a} \ln(Q^2/\Lambda^2)$$

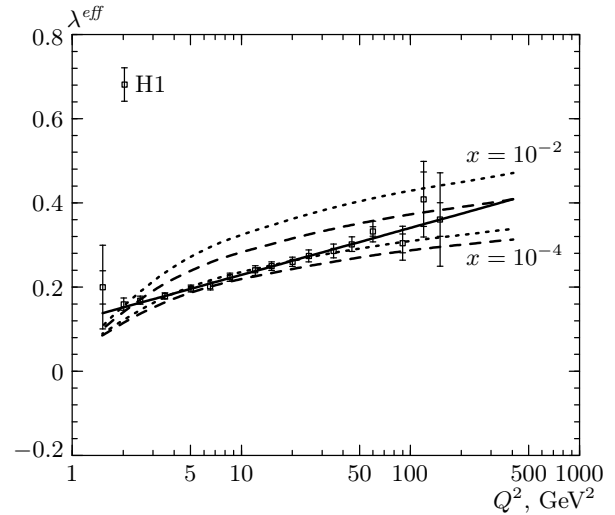


Fig. 2. The derivative $d \ln F_2 / d \ln(1/x)$ (the effective slope λ) as a function of Q^2 . Data points are from H1 [5]. Outer error bars include statistical and systematic errors added in quadrature. Inner bars correspond to statistical errors. The solid line corresponds to the H1 parameterization [5] given in Eq. (7). Dotted and dashed curves are produced as in Fig. 1. For the lower (upper) curves, the value $x = 10^{-4}$ ($x = 10^{-2}$) was used

with $C \approx 0.18$, $\hat{a} \approx 0.048$, and $\Lambda = 292 \text{ MeV}$. The linear rise of λ with $\ln Q^2$ given by Eq. (7) is plotted in Fig. 2.

As a function of x , $\lambda(Q^2)$ was found by the ZEUS Collaboration similarly. As can be seen in Fig. 8 in Ref. [4], the ZEUS data for $\lambda(Q^2)$ are compatible with a constant value of the order 0.1 at $Q^2 < 0.6 \text{ GeV}^2$, as it is expected under the assumption of a single soft Pomeron exchange within the framework of Regge phenomenology. In the case of H1, this behavior can also be inferred from the new preliminary H1 data [34] at quite low values of Q^2 .

We point out that even though our results obtained in the framework of the generalized doubled asymptotic scaling approximation (Eqs. (8)–(11) below) do not have an explicit power-like behavior, they actually mimic a power-law shape over a limited region of x and Q^2 (see Sec. 4). In addition, we have observed earlier [14] that in the generalized doubled asymptotic scaling approximation, the x dependence of the effective slopes is not strong and the F_2 effective slope is in good agreement with old (less precise) H1 data [1]. In Sec. 5, we repeat the analysis performed in Ref. [14], but with the new precise H1 data for the slope [5].

3. Q^2 -DEPENDENCE OF F_2 AND PARTON DISTRIBUTIONS IN THE GENERALIZED DOUBLED ASYMPTOTIC SCALING APPROXIMATION

We briefly recall the results of the generalized doubled asymptotic scaling approximation first presented in Ref. [14]. The small- x behavior of the parton densities and F_2 at the next-to-leading order approximation is given by³⁾

$$f_a(z, Q^2) = f_a^+(z, Q^2) + f_a^-(z, Q^2),$$

$$f_a^-(z, Q^2) \sim \exp(-d_-(1)s - D_-(1)p) + O(z), \quad (8)$$

$$f_g^+(z, Q^2) \sim I_0(\sigma) \exp(-\bar{d}_+(1)s - \bar{D}_+(1)p) + O(\rho), \quad (9)$$

$$f_q^+(z, Q^2) \sim f_g^+(z, Q^2) \left[(1 - \bar{d}_{+-}^q(1)a_s(Q^2)) \times \right. \\ \left. \times \frac{\rho I_1(\sigma)}{I_0(\sigma)} + 20a_s(Q^2) \right] + O(\rho), \quad (10)$$

$$F_2(z, Q^2) = e \left(f_q(z, Q^2) + \frac{2}{3} f_a(Q^2) f_g(z, Q^2) \right), \quad (11)$$

where

$$e = \frac{\sum_i^f e_i^2}{f}$$

is the average charge square of f effective quarks,

$$a_s = \alpha_s / 4\pi,$$

$$s = \ln \left(\frac{a_s(Q_0^2)}{a_s(Q^2)} \right), \quad p = a_s(Q_0^2) - a_s(Q^2),$$

$$D_{\pm} = d_{\pm\pm} - \frac{\beta_1}{\beta_0} d_{\pm}, \quad \sigma = 2\sqrt{(\hat{d}_+s + \hat{D}_+p) \ln z}, \quad (12)$$

$$\rho = \sqrt{\frac{(\hat{d}_+s + \hat{D}_+p)}{\ln z}} = \frac{\sigma}{2 \ln(1/z)},$$

and β_0 and β_1 are the first two terms of the QCD β -function.

The components of the leading order anomalous dimension $d_-(n)$ and the singular (\hat{d}_+) and regular ($\bar{d}_+(n)$) parts of the leading order anomalous dimension $d_+(n) = \hat{d}_+ / (n - 1) + \bar{d}_+(n)$ are given by (at $n \rightarrow 1$):

³⁾ Hereafter, $z = x/x_0$, where x_0 is a free parameter that limits the applicability range of Eqs. (8)–(11) and can be fitted from experimental data together with the magnitudes of gluon and sea quark distributions at Q_0^2 . As shown in Ref. [14], the fits to the F_2 HERA data depend very slightly on the specific x_0 value.

$$\hat{d}_+ = -\frac{12}{\beta_0}, \quad \bar{d}_+(1) = 1 + \frac{20f}{27\beta_0}, \quad (13)$$

$$d_-(1) = \frac{16f}{27\beta_0}.$$

The corresponding components in the next-to-leading order can be represented as

$$\hat{d}_{++} = \frac{412}{27\beta_0} f, \quad \hat{d}_{+-}^q = -20, \quad \hat{d}_{+-}^g = 0,$$

$$\bar{d}_{++}(1) = \frac{8}{\beta_0} \left(36\zeta_3 + 33\zeta_2 - \frac{1643}{12} + \frac{2}{9} f \left[\frac{68}{9} - 4\zeta_2 - \frac{13}{243} f \right] \right),$$

$$\bar{d}_{+-}^q(1) = 23 - 12\zeta_2 - \frac{13}{81} f, \quad \bar{d}_{+-}^g(1) = \frac{80}{81} f, \quad (14)$$

$$d_{--}(1) = \frac{16}{9\beta_0} \left(2\zeta_3 - 3\zeta_2 + \frac{13}{4} + f \left[4\zeta_2 - \frac{23}{18} + \frac{13}{243} f \right] \right),$$

$$d_{-+}^q(1) = 0, \quad d_{-+}^g(1) = -3 \left(1 + \frac{f}{81} \right).$$

Some interesting features of the results in Eqs. (8)–(12) are summarized below.

1) Both the gluon and quark singlet densities given above are presented in terms of two components («+» and «-») that are obtained from the analytic Q^2 -dependent expressions of the corresponding («+» and «-») components of parton distribution moments.

2) The «-» component is constant at small x , whereas the «+» component grows at $Q^2 \geq Q_0^2$ as $\exp \sigma$, where σ contains the positive leading-order term $|\hat{d}_+|s \ln(1/z)$ and the negative next-to-leading order one $|\hat{D}_+|p \ln(1/z)$ (see Eq. (12)). The most important part of the next-to-leading order corrections (i.e., the singular part at $x \rightarrow 0$) is therefore properly taken into account: it directly enters the argument of the Bessel functions and does not spoil the applicability of perturbation theory at low values of x .

4. Q^2 -DEPENDENCE OF THE SLOPE $d \ln F_2 / d \ln(1/x)$ IN THE GENERALIZED DOUBLED ASYMPTOTIC SCALING APPROXIMATION

Behavior of the parton densities and the structure function F_2 within the generalized doubled asymptotic scaling approach, given by Eqs. (8)–(11), can be represented by a power-law shape over a limited region of x and Q^2 [14, 15],

$$f_a(x, Q^2) \propto x^{-\lambda_a^{eff}(x, Q^2)}, \quad F_2(x, Q^2) \propto x^{-\lambda_{F_2}^{eff}(x, Q^2)}.$$

Because

$$\frac{d}{d \ln x} = \frac{d}{d \ln z},$$

the effective slopes can be obtained directly from Eqs. (8)–(11) as

$$\begin{aligned} \lambda_g^{eff}(z, Q^2) &= \frac{f_g^+(z, Q^2)}{f_g(z, Q^2)} \rho \frac{I_1(\sigma)}{I_0(\sigma)}, \\ \lambda_q^{eff}(z, Q^2) &= \frac{f_q^+(z, Q^2)}{f_q(z, Q^2)} \rho \frac{I_2(\sigma)(1 - \bar{d}_{+-}^q(1)a_s(Q^2)) + 20a_s(Q^2)I_1(\sigma)/\rho}{I_1(\sigma)(1 - \bar{d}_{+-}^q(1)a_s(Q^2)) + 20a_s(Q^2)I_0(\sigma)/\rho}, \\ \lambda_{F_2}^{eff}(z, Q^2) &= \frac{\lambda_q^{eff}(z, Q^2)f_q^+(z, Q^2) + (2f)/3a_s(Q^2)\lambda_g^{eff}(z, Q^2)f_g^+(z, Q^2)}{f_q(z, Q^2) + (2f)/3a_s(Q^2)f_g(z, Q^2)}. \end{aligned} \tag{15}$$

We emphasize that the gluon effective slope λ_g^{eff} obtained from Eq. (15) is larger than the quark slope λ_q^{eff} [14], which is in excellent agreement with Martin–Stirling–Roberts [35] and Gluck–Reya–Vogt [11] analyses (see also Ref. [10]).

On the other hand, the effective slopes λ_a^{eff} and $\lambda_{F_2}^{eff}$

in Eq. (15) depend on the magnitudes A_a of the initial parton distribution and on the chosen input values Q_0^2 and Λ . But at quite large Q^2 , where the «–» component is negligible, the dependence on the initial parton distribution disappears, and the asymptotic behavior is then given by⁴⁾

$$\begin{aligned} \lambda_g^{eff,as}(z, Q^2) &= \rho \frac{I_1(\sigma)}{I_0(\sigma)} \approx \rho - \frac{1}{4 \ln(1/z)}, \\ \lambda_q^{eff,as}(z, Q^2) &= \rho \frac{I_2(\sigma)(1 - \bar{d}_{+-}^q(1)a_s(Q^2)) + 20a_s(Q^2)I_1(\sigma)/\rho}{I_1(\sigma)(1 - \bar{d}_{+-}^q(1)a_s(Q^2)) + 20a_s(Q^2)I_0(\sigma)/\rho} \approx \\ &\approx \rho - \frac{3}{4 \ln(1/z)} + \frac{10a_s(Q^2)}{\rho \ln(1/z)}, \\ \lambda_{F_2}^{eff,as}(z, Q^2) &= \lambda_q^{eff,as}(z, Q^2) \frac{1 + 6a_s(Q^2)/\lambda_q^{eff,as}(z, Q^2)}{1 + 6a_s(Q^2)/\lambda_g^{eff,as}(z, Q^2)} + O(a_s^2(Q^2)) \approx \lambda_q^{eff,as}(z, Q^2) + \frac{3a_s(Q^2)}{\rho \ln(1/z)}, \end{aligned} \tag{16}$$

where the symbol « \approx » denotes that an approximation was made in the expansion of the modified Bessel functions $I_n(\sigma)$ ($n = 0, 1, 2$). These approximations are accurate only at large values of σ (i.e., at large Q^2 and/or small x).

Finally, we note that at the leading order, the F_2 slope $\lambda_{F_2}^{eff,as}$ is equal to the quark slope $\lambda_q^{eff,as}$ and coincides with the result in Ref. [36] for very large values of σ and a flat input (see also the first paper in Ref. [7]). At the next-to-leading order, $\lambda_{F_2}^{eff,as}$ lies between the quark and gluon slopes but closer to the former (see Fig. 3 in Ref. [14]).

5. COMPARISON WITH EXPERIMENTAL DATA

Using the results in the previous section, we have analyzed HERA data from the H1 Collaboration⁵⁾ [5] for the slope $d \ln F_2 / d \ln(1/x)$ at small x .

Initially, our results for $\lambda_{F_2}^{eff}$ depend on the five parameters Q_0^2 , x_0 , A_q , A_g , and $\Lambda_{\overline{MS}}(f = 4)$. In our previous paper [14], we fixed $\Lambda_{\overline{MS}}(f = 4) = 250$ MeV, which was a reasonable value extracted from the traditional (higher- x) experiments. All the other parameters were fitted and good agreement with the F_2 HERA data was found for $Q_0^2 \sim 1$ GeV² (all results depend on x_0 very slightly).

⁴⁾ The asymptotic formulas in Eq. (16) work quite well at any values of $Q^2 \geq Q_0^2$, because the values of λ_a^{eff} and $\lambda_{F_2}^{eff}$ are equal to zero at $Q^2 = Q_0^2$. The use of approximations in Eq. (16) instead of the exact results in Eq. (15) underestimates (overestimates) the gluon (quark) slope at $Q^2 \geq Q_0^2$ only slightly. For F_2 , the similarity of the values of $\lambda_{F_2}^{eff}$ and $\lambda_{F_2}^{eff,as}$ is shown in Fig. 1.

⁵⁾ In this paper, we only use the H1 data [5]. The preliminary ZEUS data for the slope $d \ln F_2 / d \ln(1/x)$ are only available through points in Figs. 8 and 9 of Ref. [4]. They shown quite similar properties in comparison with the H1 data [5]. Unfortunately, the ZEUS numerical values are still unavailable and we cannot analyze them in the present paper.

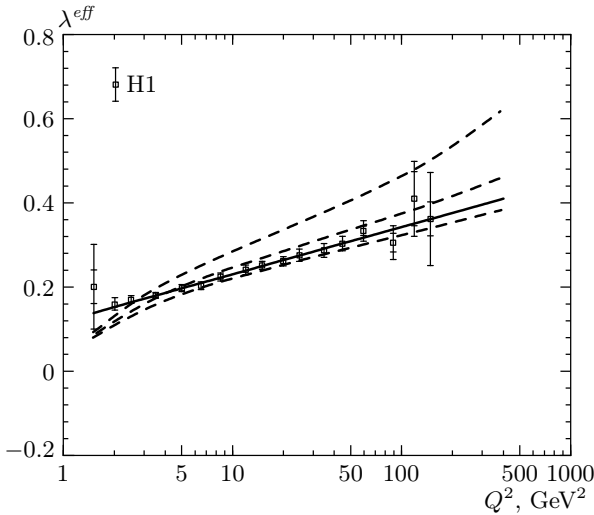


Fig. 3. The derivative $d \ln F_2 / d \ln(1/x)$ (the effective slope λ) as a function of Q^2 . Data points are from H1 [5]. Error bars and solid line are as in Fig. 2. The dashed lines were calculated via Eq. (16) using $x = a \cdot 10^{-4} Q^2$ with $a = 0.1, 1, \text{ and } 10$. Upper curves correspond to larger x

In this paper, we take $\Lambda_{\overline{MS}}(f = 4) = 292 \text{ MeV}$ in agreement with the more recent H1 results [5] and other analyses (see Ref. [37] and references therein) and we directly fit the slope $d \ln F_2 / d \ln(1/x)$ data using Eq. (15). The result is shown in Fig. 1. For comparison, we also plot the curves from a fit to the F_2 data in Ref. [14], where the value 250 MeV was used. The results are very similar and demonstrate the very important feature of an approximate x -independence of $\lambda_{F_2}^{eff}$ given by Eq. (15), which is in agreement with the H1 data [5].

Figure 1 also gives the asymptotic values for the slope $\lambda_{F_2}^{eff,as}$ obtained from Eq. (16). The agreement with the data and with the other curves is also rather good if we take in consideration that no fit is involved in this case because the only parameters entering Eq. (16) are the fixed values $\Lambda_{\overline{MS}}(f = 4) = 292 \text{ MeV}$ and $x_0 = 1$.

Thus, the extremely weak x dependence of the slope $\lambda(Q^2)$ in the considered region of x and Q^2 supports the possibility to successfully use our generalized doubled asymptotic scaling approximation in the x -independent analysis of the F_2 slope.

Figure 2 shows the experimental data for $\lambda_{F_2}^{eff}$ and the corresponding H1 parameterization [5] written above in Eq. (7). We have also plotted the result from Eqs. (16) and (15) using the parameters from our previous paper [14] as in Fig. 1. In both cases, we give

it for two representative values of x .

Visual inspection of Fig. 1 shows that the boundaries and mean values of the experimental x ranges [5] increase proportionally to Q^2 , which is related to the kinematical restrictions $x \sim 10^{-4} Q^2$ in the HERA experiments (see Refs. [1–3, 18] and, e.g., Fig. 1 in [4]).

Figure 3 shows the H1 experimental data [5] for $\lambda_{F_2}^{eff}$ and the H1 parameterization (Eq. (7)) as in Fig. 2, but this time in comparison with the asymptotic values $\lambda_{F_2}^{eff,as}$ calculated from Eq. (16) using $x = a 10^{-4} Q^2$ with $a = 0.1, 1, \text{ and } 10$. There is a reasonable agreement with the H1 data for $Q^2 > 2 \text{ GeV}^2$ with a between 0.1 and 1 (the two lower dashed curves in Fig. 3), which approximately corresponds to the middle points of the measured x range.

6. CONCLUSIONS

We have studied the Q^2 -dependence of the slope

$$\lambda_{F_2}^{eff} = d \ln F_2 / d \ln(1/x)$$

at small x in the framework of perturbative QCD. Our results are in good agreement with the new precise experimental H1 data [5] at $Q^2 \geq 2 \text{ GeV}^2$, where perturbation theory can be applicable.

Although our approach, which can be called the generalized doubled asymptotic scaling approximation, is based on pure perturbative grounds, a flat initial conditions at $Q_0^2 \approx 1 \text{ GeV}^2$ and dynamical evolution to $Q^2 \geq Q_0^2$, and is conceptually very close to the GRV approach but involves the exact analytic Q^2 -evolution, it can be reasonably applied for the new precise data of the slope $\lambda_{F_2}^{eff}$.

The agreement between $\lambda_{F_2}^{eff}$ data and perturbative QCD has already been observed by the H1 [2] and ZEUS [4] collaborations. The obtained linear rise of $\lambda(Q^2)$ with $\ln Q^2$ (see, e.g., Figs. 2 and 3), parameterized by H1 as in Eq. (7), can naively be interpreted in a strongly nonperturbative way, i.e.,

$$\lambda(Q^2) \propto \frac{1}{\alpha_s(Q^2)}.$$

Our analysis, however, demonstrates that the rise can be explained as being proportional to $\ln \ln Q^2$, which is natural in the perturbative QCD at low x (see [12–16], and references therein): when the coupling constant is running, the renormalization group leads to the small- x behavior of the parton distribution proportional to $\ln(\alpha_s(Q^2))$ at the leading order of perturbation theory and proportional to $\alpha_s(Q^2)$ at the next-to-leading order (see Eqs. (8)–(12) and discussions after Eq. (14)).

The good agreement between the perturbative QCD and the experiments obtained here and in Ref. [14, 15] demonstrates that for $Q^2 > 2 \text{ GeV}^2$, nonperturbative contributions such as shadowing effects [38], higher twist effects [39], and others either are quite small (see also Ref. [40] and references therein) or cancel between themselves and/or with $\ln(1/x)$ terms contained in the higher orders of perturbation theory. We note, however, that higher twist corrections are important at $Q^2 \leq 1 \text{ GeV}^2$, as has been demonstrated in Refs. [15, 20, 37]. Further efforts in the development of theoretical approaches are needed to isolate the correct contributions from nonperturbative dynamics and higher orders containing strong $\ln(1/x)$ terms.

Moreover, the good agreement between perturbative QCD and experimental data at low Q^2 can be explained with a larger effective scale for the QCD coupling constant [14, 15]. A similar behavior has already been observed in the framework of perturbative QCD [41] and in Brodsky–Fadin–Kim–Lipatov (BFKL) motivated approaches [42–44] (see the recent review in Ref. [45] and discussions therein).

We note that large next-to-leading order corrections calculated recently in the BFKL framework [46] (see also [47]) lead to a strong suppression of the leading-order BFKL results for the high-energy asymptotic behavior of the cross section (see, e.g., [42, 43]). A careful inclusion of the next-to-leading order corrections leads to results that are quite close to those obtained in the pure perturbative QCD [43]. This can give an additional support for the good applicability of perturbation theory in the small- x range, where, as was expected before, nonperturbative effects should give an essential contribution.

As the next step, it could be very useful to apply the generalized doubled asymptotic scaling approach to perform a combined analysis of the HERA data for F_2 , $dF_2/d\ln(Q^2)$, $d\ln F_2/d\ln(1/x)$, and F_L . We hope to consider this in a forthcoming paper, including higher-twist corrections in the Q^2 -evolution approach given by Eqs. (8)–(11). It would also be interesting to consider additional terms in the initial condition given by Eq. (1) proportional to $\ln(1/x)$ and $\ln^2(1/x)$.

We hope that this analysis will be relevant in finding the kinematical region where the well-established perturbative QCD formalism can be safely applied at small x . Moreover, the study should clear up the reason of the good agreement between the small- x relation of F_L , F_2 , and $dF_2/d\ln(Q^2)$ obtained in the pure perturbative QCD in Ref. [48] (based on previous works [26, 49]), the experimental data for these structure functions [2, 50], and the predictions in Ref. [51]

in the framework of k_t -factorization [21, 22, 52].

This paper is supported in part by the RFBR (grant № 02-02-17513), INTAS (grant № 366) and by the Heisenberg–Landau program. One of the authors (A. V. K.) was supported in part by Alexander von Humboldt fellowship during his stay in Karlsruhe University, where this paper was completed. G. P. acknowledges support of Galician research funds (PGIDT00 PX20615PR) and Spanish CICYT (FPA2002-01161).

REFERENCES

1. H1 Collab.: C. Adloff et al., Nucl. Phys. B **497**, 3 (1997).
2. H1 Collab.: C. Adloff et al., Eur. Phys. J. C **21**, 33 (2001).
3. ZEUS Collab.: S. Chekanov et al., Eur. Phys. J. C **21**, 443 (2001).
4. ZEUS Collab.: B. Surrow, E-print archives hep-ph/0201025.
5. H1 Collab.: C. Adloff et al., Phys. Lett. B **520**, 183 (2001).
6. F. J. Yndurain, *The Theory of Quark and Gluon Interactions*, 3rd edition, Berlin, Springer-Verlag (1999).
7. A. M. Cooper-Sarkar, R. C. E. Devenish, and A. De Roeck, Int. J. Mod. Phys. A **13**, 3385 (1998); C. Merino, in *Proc. of the Madagascar High-Energy Physics Int. Conf. (HEP-MAD'01)*, Antananarivo, Madagascar, ed. by S. Narison, World Scientific, E-print archives hep-ph/0201088.
8. V. N. Gribov and L. N. Lipatov, Sov. J. Nucl. Phys. **15**, 438 (1972); **15**, 675 (1972); L. N. Lipatov, Sov. J. Nucl. Phys. **20**, 94 (1975); G. Altarelli and G. Parisi, Nucl. Phys. B **126**, 298 (1977); Yu. L. Dokshitzer, Sov. Phys. JETP **46**, 641 (1977).
9. L. N. Lipatov, Sov. J. Nucl. Phys. **23**, 338 (1976); E. A. Kuraev, L. N. Lipatov, and V. S. Fadin, Phys. Lett. B **60**, 50 (1975); Sov. Phys. JETP **44**, 443 (1976); **45**, 199 (1977); Ya. Ya. Balitzki and L. N. Lipatov, Sov. J. Nucl. Phys. **28**, 822 (1978); L. N. Lipatov, Sov. Phys. JETP **63**, 904 (1986).
10. A. D. Martin, W. S. Stirling, R. G. Roberts, and R. S. Thorne, Eur. Phys. J. C **23**, 73 (2002); CTEQ Collab.: J. Pumplin et al., Preprint MSU-HEP-011101, E-print archives hep-ph/0201195.
11. M. Gluck, E. Reya, and A. Vogt, Eur. Phys. J. C **5**, 461 (1998).

12. R. D. Ball and S. Forte, Phys. Lett. B **336**, 77 (1994).
13. L. Mankiewicz, A. Saalfeld, and T. Weigl, Phys. Lett. B **393**, 175 (1997).
14. A.V. Kotikov and G. Parente, Nucl. Phys. B **549**, 242 (1999); Nucl. Phys. (Proc. Suppl.) A **99**, 196 (2001), E-print archives hep-ph/0010352; in *Proc. of the Int. Conf. PQFT98 (1998)*, Dubna E-print archives hep-ph/9810223; in *Proc. of the 8th Int. Workshop on Deep Inelastic Scattering, DIS 2000*, Liverpool (2000), p. 198, E-print archives hep-ph/0006197.
15. A. V. Kotikov and G. Parente, in *Proc. 15th Int. Seminar Relativistic Nuclear Physics and Quantum Chromodynamics*, Dubna (2000), E-print archives hep-ph/0012299; in *Proc. of the 9th Int. Workshop on Deep Inelastic Scattering, DIS 2001*, Bologna (2001), E-print archives hep-ph/0106175; in *Proc. 16th Baldin Int. Seminar Relativistic Nuclear Physics and Quantum Chromodynamics*, Dubna (2002), E-print archives hep-ph/0304064.
16. A. De Rújula et al., Phys. Rev. D **10**, 1649 (1974).
17. NM Collab.: M. Arneodo et al., Phys. Lett. B **364**, 107 (1995); Nucl. Phys. B **483**, 3 (1997); E665 Collab.: M. R. Adams et al., Phys. Rev. D **54**, 3006 (1996); A. Donnachie and P. V. Landshoff, Nucl. Phys. B **244**, 669 (1984); Nucl. Phys. B **267**, 690 (1986); Z. Phys. C **61**, 134 (1994).
18. ZEUS Collab.: J. Breitweg et al., Phys. Lett. B **407**, 432 (1997).
19. ZEUS Collab.: J. Breitweg et al., Phys. Lett. B **487**, 53 (2000); Eur. Phys. J. C **21**, 443 (2001).
20. A. Yu. Illarionov, A. V. Kotikov, and G. Parente, private communication.
21. M. Ciafaloni, Nucl. Phys. B **296**, 249 (1987); S. Catani, F. Fiorani, and G. Marchesini, Phys. Lett. B **234**, 389 (1990); Nucl. Phys. B **336**, 18 (1990); S. Catani, F. Fiorani, G. Marchesini, and G. Oriani, Nucl. Phys. B **361**, 645 (1991).
22. S. Catani, E-print archives hep-ph/9609237, in: *Proc. of the Int. Workshop on Deep Inelastic Scattering and Related Phenomena*, Rome (1996), p. 454; Z. Phys. C **75**, 665 (1997).
23. C. Lopez and F. J. Ynduráin, Nucl. Phys. B **171**, 231 (1980); Nucl. Phys. B **183**, 157 (1981).
24. V. I. Vovk, A. V. Kotikov, and S. I. Maximov, Theor. Math. Phys. **84**, 744 (1990); L. L. Jenkovszky, A. V. Kotikov, and F. Paccanoni, Sov. J. Nucl. Phys. **55**, 1224 (1992); JETP Lett. **58**, 163 (1993); Phys. Lett. B **314**, 421 (1993); A. V. Kotikov, S. I. Maximov, and I. S. Parobij, Theor. Math. Phys. **111**, 442 (1997).
25. A. V. Kotikov, Phys. Atom. Nucl. **56**, 1276 (1993).
26. A. V. Kotikov, Phys. Atom. Nucl. **57**, 133 (1994); Phys. Rev. D **49**, 5746 (1994).
27. A. V. Kotikov, Mod. Phys. Lett. A **11**, 103 (1996); Phys. Atom. Nucl. **59**, 2137 (1996).
28. C. Lopez, F. Barreiro, and F. J. Ynduráin, Z. Phys. C **72**, 561 (1996); K. Adel, F. Barreiro, and F. J. Ynduráin, Nucl. Phys. B **495**, 221 (1997).
29. A. Donnachie and P. V. Landshoff, Phys. Lett. B **296**, 227 (1992); Phys. Lett. B **437**, 408 (1998).
30. H. Abramowitz, E. M. Levin, A. Levy, and U. Maor, Phys. Lett. B **269**, 465 (1991); A. Levy, DESY preprint 95-003 (1995), E-print archives hep-ph/9501346.
31. G. M. Frichter, D. W. McKay, and J. P. Ralston, Phys. Rev. Lett. **74**, 1508 (1995).
32. A. Capella, A. B. Kaidalov, C. Merino, and J. Tran Thanh Van, Phys. Lett. B **337**, 358 (1994); A. B. Kaidalov, C. Merino, and D. Pertermann, Eur. Phys. J. C **20**, 301 (2001).
33. P. Desgrolard, L. L. Jenkovszky, and F. Paccanoni, Eur. Phys. J. C **7**, 655 (1999).
34. H1 Collab.: T. Lastovicka, in: *Proc. of the Int. Workshop on Deep Inelastic Scattering*, Cracow (2002); H1 Collab.: J. Gayler, in: *Proc. of the Int. Workshop on Deep Inelastic Scattering*, Cracow (2002).
35. A. D. Martin, W. S. Stirling, and R. G. Roberts, Phys. Lett. B **387**, 419 (1996).
36. H. Navelet, R. Peshanski, Ch. Royon, L. Schoeffel, and S. Wallon, Mod. Phys. Lett. A **12**, 857 (1997).
37. V. G. Krivokhijine and A. V. Kotikov, JINR preprint E2-2001-190, E-print archives hep-ph/0108224; in: *Proc. of the 16th Int. Workshop on High Energy Physics and Quantum Field Theory*, Moscow (2001), E-print archives hep-ph/0206221; Acta Phys. Slov. **52**, 227 (2002); Acta Phys. Polon. B **33**, 2947 (2002); Nucl. Instrum. Meth. A **502**, 624 (2003).
38. E. M. Levin, E-print archives hep-ph/9706341, hep-ph/9706448, in: *Proc. of the Int. Workshop on Deep Inelastic Scattering*, Chicago (1997).
39. J. Bartels and C. Bontus, in: *Proc. of the Int. Workshop on Deep Inelastic Scattering*, Chicago (1997); A. D. Martin and R. S. Thorne, preprint DTP/98/04, E-print archives hep-ph/9802366; J. Bartels, in: *Proc. of the Int. Workshop on Deep Inelastic Scattering*, Cracow (2002).

40. J. Bartels, K. Golec-Biernat, and K. Peters, *Eur. Phys. J. C* **17**, 121 (2000); K. Golec-Biernat, in: *Proc. of the Int. Workshop on Deep Inelastic Scattering, Cracow* (2002).
41. Yu. L. Dokshitzer and D. V. Shirkov, *Z. Phys. C* **67**, 449 (1995); A. V. Kotikov, *JETP Lett.* **59**, 1 (1994); *Phys. Lett. B* **338**, 349 (1994); W. K. Wong, *Phys. Rev. D* **54**, 1094 (1996).
42. S. J. Brodsky, V. S. Fadin, V. T. Kim, L. N. Lipatov, and G. B. Pivovarov, *JETP Lett.* **70**, 155 (1999); V. T. Kim, L. N. Lipatov, and G.B. Pivovarov, in: *Proc. of the 8th Blois Workshop at IHEP, Protvino* (1999), preprint IITAP-99-013, E-print archives hep-ph/9911228; in: *Proc. of the Symp. on Multiparticle Dynamics (ISMD99)*, Providence, Rhode Island (1999), preprint IITAP-99-014, E-print archives hep-ph/9911242.
43. S. J. Brodsky, V. S. Fadin, V. T. Kim, L. N. Lipatov, and G. B. Pivovarov, in: *Proc. of the PHOTON2001, Ascona, Switzerland* (2001), preprint CERN-TH/2001-341, SLAC-PUB-9069, E-print archives hep-ph/0111390.
44. M. Ciafaloni, D. Colferai, and G. P. Salam, *Phys. Rev. D* **60**, 114036 (1999); *JHEP* **07**, 54 (2000); R. S. Thorne, *Phys. Lett. B* **474**, 372 (2000); *Phys. Rev. D* **60**, 054031 (1999); *Phys. Rev. D* **64**, 074005 (2001); G. Altarelli, R. D. Ball, and S. Forte, *Nucl. Phys. B* **621**, 359 (2002).
45. Bo Andersson et al., *Eur. Phys. J. C* **25**, 77 (2002).
46. V. S. Fadin and L. N. Lipatov, *Phys. Lett. B* **429**, 127 (1998); G. Camici and M. Ciafaloni, *Phys. Lett. B* **430**, 349 (1998);
47. A. V. Kotikov and L. N. Lipatov, *Nucl. Phys. B* **582**, 19 (2000); in: *Proc. of the 35th Winter School, Repino, S'Peterburg* (2001), E-print archives hep-ph/0112346; *Nucl. Phys. B* **661**, 19 (2003).
48. A. V. Kotikov, *JETP* **80**, 979 (1995); A. V. Kotikov and G. Parente, in: *Proc. of the Int. Workshop on Deep Inelastic Scattering and Related Phenomena, Rome* (1996), p. 237, E-print archives hep-ph/9608409; *Mod. Phys. Lett. A* **12**, 963 (1997); *JETP* **85**, 17 (1997).
49. A. V. Kotikov, *JETP Lett.* **59**, 667 (1994); A. V. Kotikov and G. Parente, *Phys. Lett. B* **379**, 195 (1996).
50. H1 Collab.: N. Gogitidze, *J. Phys. G* **28**, 751 (2002).
51. A. V. Kotikov, A. V. Lipatov, and N. P. Zotov, *Eur. Phys. J. C* **27**, 219 (2003).
52. S. Catani, M. Ciafaloni and F. Hautmann, *Phys. Lett. B* **307**, 197 (1993); S. Catani and F. Hautmann, *Phys. Lett. B* **315**, 157 (1993); *Nucl. Phys. B* **427**, 472 (1994).